Synthetic Metals 159 (2009) 513–517

Contents lists available at ScienceDirect

Synthetic Metals

journal homepage: www.elsevier.com/locate/synmet

Suitability of 3,4-dialkyl substitution in molecular crystal based on thiophene–fluorenone for organic field effect transistors

W. Porzio[a,*], S. Destri[a], M. Pasini[a], U. Giovanella[a], R. Resel[b], O. Werzer[b], G.Scavia[c], L. Fumagalli[d], D. Natali[d], M. Sampietro[d]

[a] Istituto per lo Studio delle Macromolecole, C.N.R., via E. Bassini 15, 20133 Milano, Italy
[b] Institute of Solid State Physics, Graz University of Technology, Petersgasse 16, A-8010 Graz, Austria
[c] Istituto di Struttura della Materia, CNR, via Salaria Km 29, 500 00016 Monterotondo Scalo, Italy
[d] Dipartimento di Elettronica e Informazione Politecnico di Milano P.za L. da Vinci 32, 20133 Milano, Italy

ARTICLE INFO

Article history:
Received 12 February 2008
Received in revised form 13 June 2008
Accepted 21 November 2008
Available online 3 January 2009

PACS:
81.05.Lg
83.80.Xz
85.30.Tv

Keywords:
Substituted oligomer
Liquid crystal
FET

ABSTRACT

A new co-oligomer constituted by both a thiophene sequence bearing a 3,4-dialkyl substitution, imparting processability, and by end-capping fluorenone moieties, has been synthesised. The molecule, potentially suitable for close-packing aptness, has been characterized by means of combined optical, thermal, structural, and morphological analyses, showing that, despite the O–H intermolecular interaction favoured by fluorenone presence, the large steric hindrance specific to the dialkyl 3,4-disubstitution strongly limits the intermolecular interaction. Hence it makes such substitution pattern unsuitable for field effect transistor application, as it is confirmed by the electrical performances measured on prototype devices.

1. Introduction

In the topic of field effect transistors based on organic layers (OFET) huge efforts have been made to address peculiar issues of these materials, namely electronic level matching with the electrodes, close packing of conjugated units, e.g. π-stacking, crystal size in the films, and proper with respect to the substrate orientations among the others [1–7].

In spite of the up to date quite interesting results attained [3,4,6,7], clear structure–property relationships are still missing in many cases. In this contribution, we focus on the role of multi-β-alkyl substitution onto conjugated segments, on the mobility of OFET structures. In particular, it has been recently shown that the 3,4-disubstitution with alkyl chains at the thiophene ring, though convenient because it imparts processability and can prevent the π-dimerization of cation radical [8], is unfavourable to charge transport due to intermolecular steric interactions that prevent an effective electronic overlap [8].

Moreover the role of fluorenone moiety in FET devices has been studied [9–11], indicating a remarkable close-packing aptness.

Our aim is to explore the possibility to counter balance the effect of alkyl 3,4-disubstitution, i.e. processability [12,13] and steric hindrance, by end-capping the thiophene sequence with fluorenone moieties, which are known to be able to induce close packing thanks to oxygen–hydrogen interactions. The molecular structure of designed oligomer (hereinafter **1**) is sketched in Scheme 1.

The paper shows that, even in presence of fluorenone, it is not possible to reach an efficient molecular stacking favourable to charge transport.

2. Synthesis and electrochemical characterisation

Molecule **1**, i.e. 5,5‴″-(2-fluorenon-2-yl)-3′,4′,3‴″,4‴″-tetrahexylsexithiophene, was prepared by dimerisation of 5-(2-fluorenon-2-yl)-3′,4′-dihexyl-2,2′;5′,2″-terthiophene (hereinafter **2**) obtained by Suzuki coupling [9] of 5-(4,4,5,5-tetramethyl-1,3,2-dioxoborolane-2yl)-3′,4′-dihexyl-2,2′;5′,2″-terthiophene with 2-bromofluorenone. The electrochemical synthesis and the molecular characterization of **1** are reported in Ref. [14]; here we underlay the cyclovoltammetry experiments carried out on **1** in order to derive the highest occupied molecular orbital (HOMO)

* Corresponding author. Tel.: +39 0223 699371; fax: +39 0270 636400.
E-mail address: w.porzio@ismac.cnr.it (W. Porzio).

0379-6779/$ – see front matter © 2008 Elsevier B.V. All rights reserved.
doi:10.1016/j.synthmet.2008.11.017

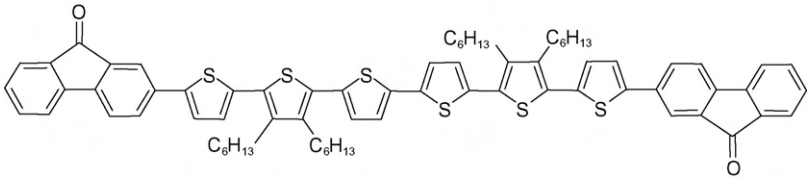

Scheme 1. Chemical structure of **1**.

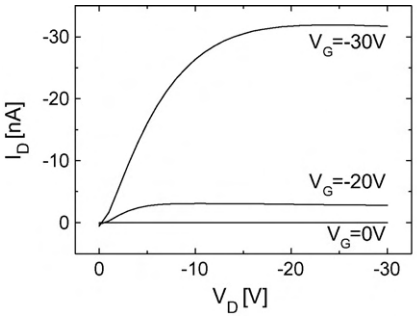

L [μm]	μ [cm^2/Vs]	I_{ON}/I_{OFF}
3	$1.4 - 1.7 \times 10^{-5}$	$2.8 \times 10^4 - 1.5 \times 10^5$
6	$0.8 - 1.0 \times 10^{-5}$	$4.2 - 7.6 \times 10^3$
12	0.6×10^{-5}	2.3×10^3

Fig. 1. Output characteristic curves for **1** spin-cast from chloroform solution (left), and extracted parameters (right).

level that is fundamental to determine its matching with gold electrode work-function.

The cyclic voltammogram (CV) of **1** shows two reversible oxidation processes, centered at $E_0 = 0.22$ V and 0.52 V, followed by a further flat oxidative process with capacitive properties starting from ca. 0.9 V (see supplementary material). As for sexithiophenes the first two peaks correspond to an overall two electron oxidation; this suggestion has been confirmed by EQCM analysis relating charge and dry mass. The related reduction occurred at $E_0 = -1.70$ V. The calculated E_g and HOMO values, using the method described in Ref. [15], are close to 1.92 eV and 4.94 eV respectively. Therefore no significant injection barriers in our OFET structure which employ platinum (work function 5.65 eV) source and drain contacts are expected.

2.1. FET measurements

Attempts to deposit molecule **1** by thermal evaporation were unsuccessful because decomposition occurred before film growth could start. Therefore we reverted to deposition from solution. When spin-coated from tetrachloroethane (TCE), **1** has a mobility of about $(1–5) \times 10^{-6}$ $cm^2/(V\,s)$ and on/off ratio in the range of a

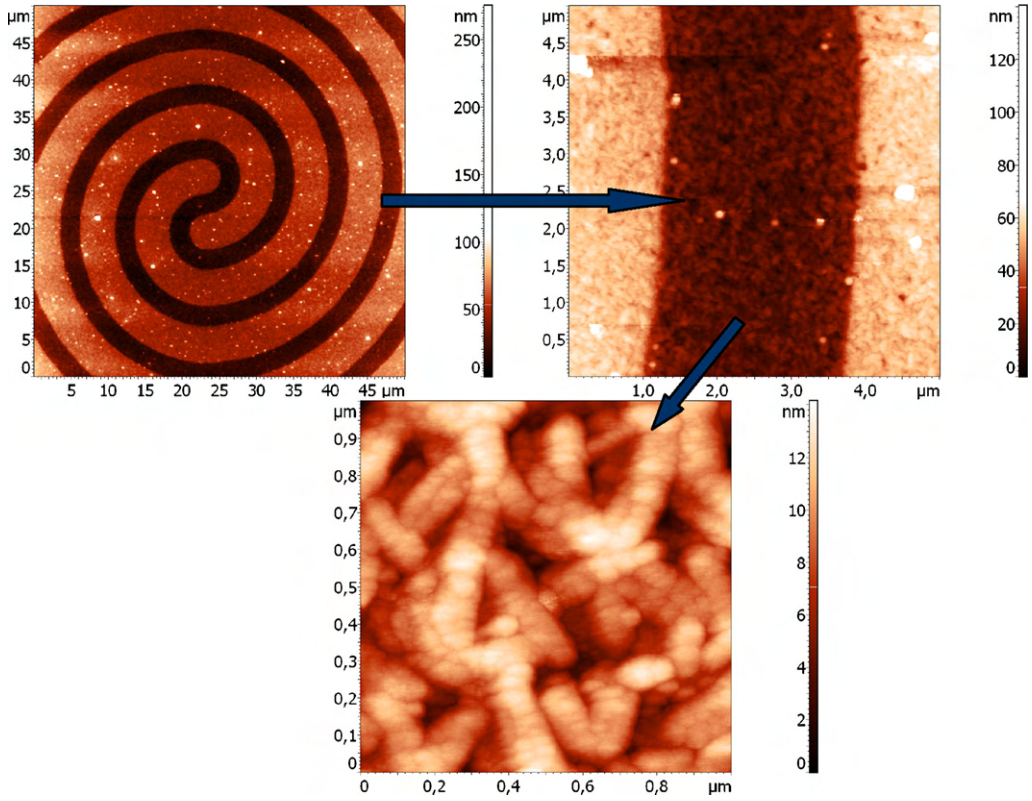

Fig. 2. AFM height images of OFET device based on **1** molecule spin-cast from $CHCl_3$.

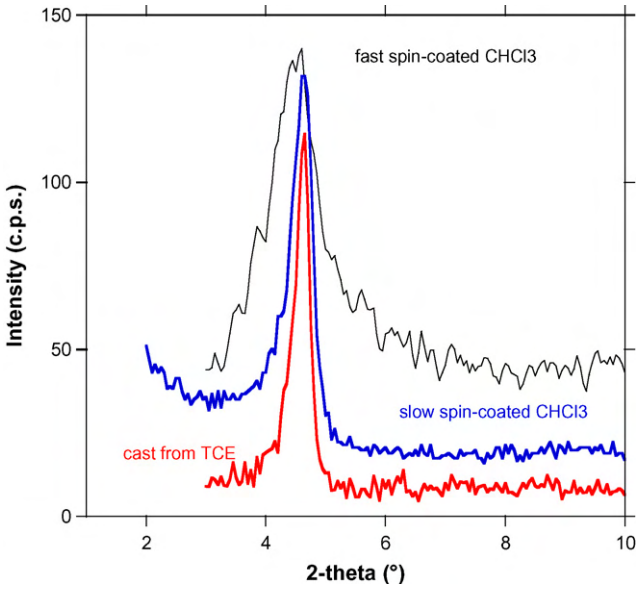

Fig. 3. XRD patterns of thin films of molecule **1** obtained in different conditions, the spectra are limited to significant region.

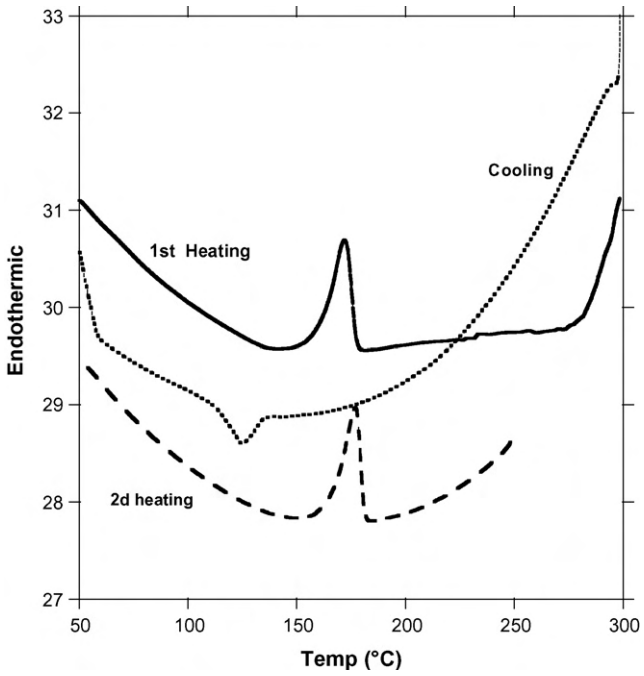

Fig. 5. DSC traces of molecule I powders under dry N_2.

few tens. Better results in terms of mobility are obtained by casting from TCE ($(1–7)\times 10^{-5}$ cm^2/(V s)), but with on/off ratio below ten. When spin-coated from chloroform solution, **1** gives an average mobility of about 10^{-5} cm^2/(V s) with on/off ratio between 10^3 and 10^5 (Fig. 1); efforts to enhance the mobility by annealing were unsuccessful leading to a reduction of the mobility by a factor of 2.

To investigate the origin of the relatively poor performance of the molecule, the morphology of the film was investigated by means of AFM. In Fig. 2 the height images at different magnification levels on a 3 μm long channel length, in a device prepared by CHCl3 spin coating, are reported.

The ultimate morphological units (globular-like) do not exceed 30 nm, while the domain coherence length (interlayer spacing) in films cast from TCE solution, as derived from XRD profile analysis [16], reaches approximately 25 nm (see below). Therefore, balancing between incomplete coverage in cast films and more homogeneous, but less crystalline spin-coated films, it is unlikely that morphology, at least in terms of substrate coverage in spin-coated films, is the leading factor in limiting the mobility. In fact, although the domain size as derived from film XRD patterns are different according to preparation conditions, as shown in Fig. 3, other thiophene-based oligomers display larger mobility values, in spite of the reduced domain size [17]. In this view, the optical, thermal, and structural analyses are carried on attempting to rationalize the mobility behaviour of molecule **1**.

2.2. Optical characterisation

In Fig. 4 the absorption and photoluminescence spectra of both solutions and cast films are presented. From the absorption edge (of solid-state) an E_g value near to 2.05 eV is derived in reasonable agreement with the electrochemically derived one.

No evidence of H-aggregate formation in solid-state [18] is obtained by optical characterization; this observation suggests that a real close-packed organization is prevented, i.e. the π-stacking of conjugated segments is somewhat weaken, as already observed in

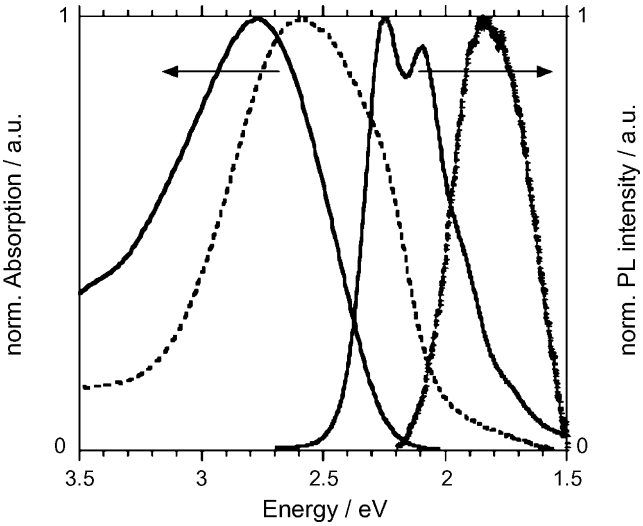

Fig. 4. Normalized absorption and PL spectra of solution (solid line) and cast-film (dotted line).

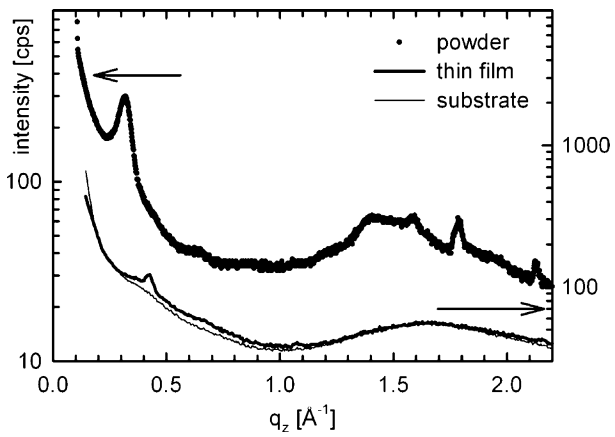

Fig. 6. Diffraction pattern of the powder as well as a specular scan of a thin film sample. The background of the glass substrate of the thin film is drawn by a thin full line, the intensity scales for the powder and the thin film diffraction pattern are on the left or right side, respectively.

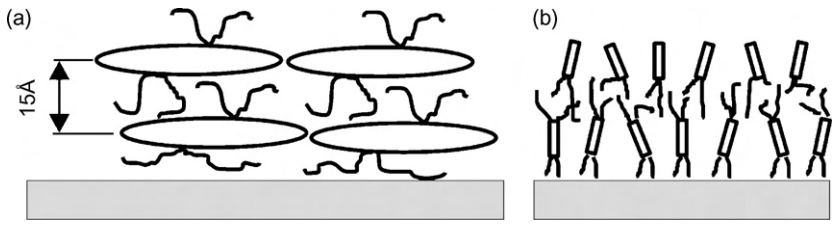

Fig. 7. Schematic picture of the orientation and of the molecules relative to the substrate surface is a side view (a) and in a front view (b).

disubstituted oligomers [8]. Nevertheless, the aggregation reached is enough to quench almost completely the luminescence, in fact the photoluminescence quantum yield, measured with integrated sphere, does not exceed 1% for film spin-cast either from $CHCl_3$ or TCE.

2.3. Thermal characterisations

Differential scanning calorimetry (DSC) analysis was performed onto crystalline powders under dry nitrogen in Fig. 5 the resulting traces are reported. In the first heating scan an endothermic peak appears centred at 172 °C (ΔH = 23.1 J/g) attributable to phase transition from 3D to nematic arrangement, see below the XRD characterisation. No other peaks are detected up to 300 °C, the cooling trace reveals an exothermic peak centred at 125 °C (ΔH = 19.1 J/g) attributable to incomplete crystallisation into 3D phase. A further heating scan confirms the solid–solid transition previously observed, centred at 175 °C (ΔH = 20.9 J/g). It should be mentioned that in several cases molecular crystals show evident phase transition with large enthalpies while the melting event is either hardly observable or undetected; indeed the transition from nematic to liquid phase implies small energy [19]. The observations in polarized microscopy in the temperature range 25–300 °C is fully in agreement with DSC findings. Thermogravimetric analysis carried out under dry N_2 reveals a substantial stability over 360 °C (weight loss < 3%).

2.4. XRD characterisation and modelling

The X-ray diffraction pattern of the powder sample is depicted in Fig. 6. A dominant diffraction peak occurs at $q = 0.33\ Å^{-1}$; in addition, an amorphous halo is present at around $q = 1.5\ Å^{-1}$ and a peak is observed at $1.8\ Å^{-1}$, which will be discussed later. The fact that diffraction peaks as well as an amorphous halo are present reveals the semicrystalline nature of the material in the as-prepared state. In the thin film sample, prepared either by spin-coating or by casting from low-boiling point solvents, the powder peaks are unobserved, whereas a single peak appears at $q = 0.42\ Å^{-1}$. The shift of the first strong diffraction peak from $q = 0.33\ Å^{-1}$ observed in the powder sample to $q = 0.42\ Å^{-1}$ in the thin film reveals that a polymorph phase is present within the thin film. The preferred orientation of the ordered state in the thin film was determined by ψ-scans at fixed $q = 0.42\ Å^{-1}$, which show a width of $20° \pm 5°$. The presence of a finite rocking width at $q = 0.42\ Å^{-1}$ means that planes with a repeating distance of 15.0 Å are arranged parallel with respect to the substrate. The conjugated backbone of the molecule has a van der Waals length of 42 Å which is quite different from the observed interplanar distance of 15.0 Å: this difference shows that the backbones of the molecules cannot be oriented in a perpendicular manner to the surface of the substrate, as it is common for rod-like or β-alkyl substituted molecules [19–21], and α–ω hexyl-substituted thiophene-based molecules [22]. On the contrary, the observed distance of 15.0 Å suggests that the long molecular axes are aligned parallel to the substrate. It has to be clarified whether **1** adopts a *face-on* or an *edge-on* configuration. The former situation should reveal the characteristic distance for stacking of aromatic units, but this would be around 3.5 Å, as it is suggested by the powder pattern which shows a strong diffraction peak at $q = 1.8\ Å^{-1}$ (d = 3.5 Å), although relatively broad.

As the observed distance is 15.0 Å, the face-on configuration is ruled out and we conclude that the long molecular axes are aligned edge-on with respect to the substrate surface, as it is observed for conjugated oligomers [23] and polymers with analogous hexylic side-chains, namely poly(3-hexylthiophene) [24,25]. Fig. 7 gives a schematic drawing of the arrangement of the molecules relative to the substrate surface. The conjugated backbones of the molecules are aligned parallel to the substrate surface (Fig. 7a) and the backbones pack parallel to each other (Fig. 7b). Spin-coated films used for prototypes of FET device, gave XRD pattern similar to that shown in Fig. 5, i.e. only one relatively broad peak, indicating the nematic arrangement achieved by the molecule. These observations leads us to conclude that the close-packing *potentially* induced by C=O residue is hindered by the individual conformations of the molecular backbones: due to the 3-4-hexyl disubstitution at the thiophene ring, the flexible side chains suffer from a mutual steric hindrance and hence fill the open space in a disordered way.

3. Conclusions

A new conjugated oligomer, thought to impart to a thiophene sequence with alkyl 3,4-disubstitution a potential close-packed arrangement thanks to end-capping with fluorenone moieties, has been extensively studied. XRD analyses shows that the molecule adopts an edge-on configuration, similar to poly(3-hexylthiophene)one, and that, notwithstanding the presence of fluorenone moieties, the potential close packing of conjugated sequences (π-stacking) is partially hampered by intermolecular steric interactions due to alkyl 3,4-disubstitution of thiophene rings [8]. This is in agreement with optical characterizations, indicating luminescence quenching, i.e. aggregation, but exciton interaction lacking. These analyses fully account for the performances in OFET structures, namely the relatively low mobility in the range of few $10^{-5}\ cm^2/(V\,s)$ and an I_{on}/I_{off} ratio of 10^2. In conclusion, the 3,4-disubstitution pattern proves to be unfavourable to close packing arrangement and hence unsuitable for OFET application of organic molecules.

4. Experimental

Thin films of molecule **1** were prepared by spin-coating of TCE solution ($10\ mg/cm^3$) or chloroform solution at ($8\ mg/cm^3$), spun at 1500 rpm, and by casting from TCE solution ($10\ mg/cm^3$). The thermal treatment was performed at 140 °C for 15 min in vacuum at 10^{-7} mbar, followed by slow cooling down to 30 °C.

Electrochemical experiments were performed at room temperature under nitrogen in three electrode cells. The counter electrode was platinum; reference electrode was a silver/0.1 M silver perchlorate in reagent grade (Uvasol, Merck) acetonitrile with a water content ≤0.01% (0.34 V vs. Standard Calomelan Elec-

trode); the working electrode was a platinum minidisc electrode (0.003 cm^2); the supporting electrolyte was tetrabutylammonium perchlorate and was previously dried under vacuum at 70 °C.

The cyclic voltammogram of **2** was performed in 1:1 acetonitrile/CH_2Cl_2 + 0.1 M Bu_4NClO_4, as the molecule is scarcely soluble in acetonitrile alone. Bulk dimer has been produced by exhaustive electrolysis (1.5 F mol^{-1}) at 0.7 V of 23 mg of **2** in 25 ml 1:1 acetonitrile/CH_2Cl_2 + 0.1 M Bu_4NClO_4. The resulting green suspension of the radical cation form has been reduced with hydrazine to a red-orange precipitate which was filtered off, washed with acetonitrile and dried.

X-ray diffraction was performed with a Philips X'Pert system equipped with an ATC3 texture cradle serving an Eulerian geometry. A Bragg–Brentano focussing geometry was employed in combination with a graphite monochromator on the secondary side; Cr Kα radiation was used. The diffraction pattern of the powder as well as the specular scan of the thin film samples was performed by $\Theta/2\Theta$-scans. The powder was used in the as prepared state and prepared on inclined cutted silicon crystals to get low experimental background. The mosaicity of the thin films were determined by ψ-scans with ψ as the tilt angle of the scattering vector out of the coplanar direction of the primary and the scattered beam. AFM investigations were performed using a NT-MDT NTEGRA apparatus in tapping mode. FET devices have been realized in bottom contact configuration, with platinum source and drain contacts defining channel lengths of 3, 6, and 12 μm, lithographed onto a 1300 Å thick SiO_2 acting as the gate dielectric. SiO_2 was functionalized with dimethyldichlorosilane prior to molecule deposition.

Measurements have been performed at about 10^{-5} mbar. TFT parameters have been extracted from the saturation region (gate to source voltage −30 V, drain to source voltage −30 V).

Acknowledgements

This paper has been partially supported by Fondazione CARIPLO under the project PROTEO. We thank Dr. G. Zotti for both cyclovoltammetric characterisation and electrosynthesis and J. Ahmad for assisting the performance of XRD measurements.

Appendix A. Supplementary data

Supplementary data associated with this article can be found, in the online version, at doi:10.1016/j.synthmet.2008.11.017.

References

[1] H. Sirringhaus, N. Tessler, R.H. Friend, Science 280 (1998) 1741.
[2] C.D. Dimitrakopoulos, P.R.L. Malenfant, Adv. Mater. 14 (2002) 99.
[3] S. Forrest, Nature 428 (2004) 911.
[4] (a) A. Facchetti, M.H. Yoon, T.J. Marks, Adv. Mater. 17 (2005) 1705; (b) A. Facchetti, Mater. Today 10 (2007) 28.
[5] J. Cao, J.W. Kampf, M.D. Curtis, Chem. Mater. 15 (2003) 404.
[6] (a) G. Horowitz, Adv. Mater. 10 (1998) 365; (b) G. Horowitz, J. Mater. Chem. 9 (1999) 2021.
[7] A.R. Murphy, J.M.J. Freĭchet, Chem. Rev. 107 (2007) 1066.
[8] C. Videlot, J. Ackermann, P. Blanchard, J.-M. Raimundo, P. Frere, M. Allain, R. De Bettignies, E. Levillain, J. Roncali, Adv. Mater. 15 (2003) 306.
[9] W. Porzio, S. Destri, M. Pasini, U. Giovanella, T. Motta, M.D. Iosip, D. Natali, M. Sampietro, L. Franco, M. Campione, Synth. Met. 146 (2004) 259.
[10] C. Chi, C. Im, V. Enkelmann, A. Ziegler, G. Lieser, G. Wegner, Chem. A: Eur. J. 11 (2005) 6833.
[11] F. Jaramillo-Isaza, M.L. Turner, J. Mater. Chem. 16 (2006) 83.
[12] H. Sirringhaus, Adv. Mater. 17 (2005) 2411.
[13] R. Zhang, B. Li, M.C. Iovu, M. Jeffries-EL, G. Sauveĭ, J. Cooper, S. Jia, S. Tristram-Nagle, D.M. Smilgies, D.N. Lambeth, R.D. McCullough, T. Kowalewski, J. Am. Chem. Soc. 128 (2006) 3480.
[14] G. Zotti, S. Zecchin, B. Vercelli, M. Pasini, S. Destri, F. Bertini, A. Berlin, Chem. Mater. 18 (2006) 3151.
[15] S. Janietz, D.D.C. Bradley, M. Grell, M. Giebeler, M. Inbasekaran, E.P. Woo, Appl. Phys. Lett. 73 (1998) 2453.
[16] S. Enzo, G. Fagherazzi, A. Benedetti, S. Polizzi, J. Appl. Cryst. 21 (1988) 536.
[17] W. Porzio, S. Destri, U. Giovanella, M. Pasini, T. Motta, D. Natali, M. Sampietro, M. Campione, Thin Solid Films 492 (2005) 212.
[18] Y. Sun, Y. Ma, Y. Liu, Y. Lin, Z. Wang, Y. Wang, C. Di, K. Xiao, X. Chen, W. Qiu, B. Zhang, G. Yu, W. Hu, D. Zhu, Adv. Funct. Mater. 16 (2006) 426.
[19] S. Destri, M. Mascherpa, W. Porzio, Adv. Mater. 5 (1993) 43, and ref. therein.
[20] K. Erlacher, R. Resel, J. Keckes, F. Meghdadi, G. Leising, J. Cryst. Growth 206 (1999) 135.
[21] A. Borghesi, A. Sassella, R. Tubino, S. Destri, W. Porzio, Adv. Mater. 10 (1998) 931.
[22] F. Garnier, A. Yassar, R. Hajlaoui, G. Horowitz, F. Deloffre, B. Servet, S. Ries, P. Alnot, J. Am. Chem. Soc. 115 (1993) 8716.
[23] J. Roncali, Macromol. Rapid Commun. 28 (2007) 1761.
[24] (a) T.J. Prosa, M.J. Winokur, J. Moulton, P. Smith, A.J. Heeger, Macromolecules 25 (1992) 4364; (b) A. Bolognesi, W. Porzio, G. Zhuo, T. Ezquerra, Eur. Pol. J. 32 (1996) 1097.
[25] A. Zen, M. Saphiannikova, D. Neher, J. Grenzer, S. Grigorian, U. Pietsch, U. Asawapirom, S. Janietz, U. Scherf, I. Lieberwirth, G. Wegner, Macromolecules 39 (2006) 2162.